scientific reports

Check for updates

OPEN

Study on energy absorption of paper honeycomb sandwich tube filled by polyethylene foam under axial loading

Xuefei Du[1,3]✉, Yanfeng Guo[2]✉, Yungang Fu[2], Xuxiang Han[2] & Qing Wei[2]

This work proposed an approach to multi-component non-metallic materials, namely regular polygonal paper honeycomb sandwich tubes filled with polyethylene (PE) foam, and focused on the influence of drop impact parameters and structural parameters on the deformation characteristics and energy absorption of the filled tubes. Axial drop impact tests were employed to exert drop impact loading on cross-sections of the specimens with a square drop weight. The results showed that the X-direction filled tube (X-DFT) had a higher crushing strength and yield strength than that of the Y-direction filled tube (Y-DFT). As the tubular cross-section edge number of the filled tube increased, the specific energy absorption (SEA) and specific total efficiency (STE) decreased. Under the same axial drop impact loading conditions, the SEA and STE of the X-DFT were superior to those of the Y-DFT. As the edge number of the tubular cross-section or the tubular length ratio increased, the SEA and STE of the filled honeycomb tube decreased significantly. While the impact energy increased, the SEA and STE of the filled tubes increased approximately linearly. This work investigated the influence of drop-impact and structural parameters on deformation characteristics and energy absorption. It is expected to provide supplementary documentation for the advancement of cushion protection technology and the optimization of product structure.

Keywords Sandwich tube, Paper honeycomb, Polyethylene foam, Compression deformation, Axial drop impact, Energy absorption

Currently, the compressive properties[1] and crashworthiness characteristics[2] of composite structures[3] are a hot field. The energy absorption of the composite structure can be a significant improvement[4] by filling polyethylene foam and paper honeycomb materials. The carrying capacity and impact resistance of laminated tubular structures have been enhanced through the combined effect of corrugation/honeycomb structures and polymer foam[5,6].

Recent studies on composite structures showed that thin-walled polygonal tubes enhance energy absorption by increasing the edges of the tube cross-section and the number of folding units, the multi-cell method can be beneficial in improving the axial compression performance and energy-absorbing capacity of polygonal tubes[7,8]. Dehghanpour[1,9] investigated the energy absorption capacities and deformations of thin-walled tubes with different section geometries and metal matrix composite tubes under quasi-static loading. Taghipoor[10] studied the energy absorption and collapse behaviors of composite corrugation cylindrical absorbers. Eyvazian et al.[11] investigated the crushing behaviors and energy-absorbing of an aluminum circular tube with deep and shallow corrugation. Liu et al.[12] studied corrugated aluminum circular tubes with longitudinal sinusoidal patterns and explored the effect of corrugation parameters on dynamic buckling under axial impact loading. Yuan et al.[13] and Ye et al.[14] investigated the shape deformation, energy-absorbing mechanism, and optimal design of the square/rectangular/hexagonal crash-resistant copper box, as well as pentagon/hexagon/ heptagon/octagon carbon fiber composite material tube under axial load. Scholars proposed that the sandwich tube be filled with foam material facilitate to influencing energy absorption capacity. Taghipoor[15] studied the energy absorption effect of foam-filled corrugated core sandwich panels. Goyal et al.[16] investigated the energy-absorbing characteristics of

[1]School of Materials Science and Engineering, Jiujiang University, Jiujiang 332005, Jiangxi, People's Republic of China. [2]Department of Packaging Engineering, Xi'an University of Technology, Xi'an 710048, Shaanxi, People's Republic of China. [3]Jiangxi Province Engineering Research Center of Materials Surface Enhancing and Remanufacturing, School of Mechanical and Materials Engineering, Jiujiang University, Jiujiang 332005, People's Republic of China. ✉email: dxfawl@163.com; 272967642@qq.com; guoyf@xaut.edu.cn

octagonal star-shaped aluminum/steel tubes filled with polyurethane and polystyrene foam under axial dynamic compression. Kilicaslan et al.[17], their study of foam-filled longitudinal sinusoidal corrugated aluminum circular tubes and corrugated outer/inner circular tubes showed that the axial dynamic crushing responses of corrugated tubes included an accordion collapse mode, a concertina progressive collapse mode, and a diamond collapse mode. Huang et al.[18] studied the energy absorption properties of composite sandwich tubes with pre-folded cores, and their energy absorption performance was better than the stand-alone tubes or tubes with corrugated cores. Zhang et al.[19] studied the dynamic impact response characteristics of polypropylene (PP) foam–filled honeycomb aluminum through experiments and simulations. These works all showed that polymer-filled honeycomb structures have enhanced energy-absorbing capacity and load-bearing performance.

Numerous previous studies have concentrated on the mechanical and construction of rigid components, particularly in the context of metal materials. In the field of cushioning protection, the research on the structure and cushioning energy absorption of non-metallic materials remains an area in need of further investigation. Referring to the design concepts of the foam-filled tube, corrugation tube, and sandwich tube, the authors propose a novel approach to multi-component non-metallic materials, namely a paper honeycomb sandwich tube filled with polyethylene (PE) foam. The potential applications of the proposed structures can serve as energy-absorbing components and enhance the impact protection capability of products in the environments of distribution and employment in the field of transport safety and cushion protection. The investigation focuses on the drop-impact and structural parameters of deformation characteristics and energy absorption capacity of sandwich tubes. It is expected that this study could provide supplementary documentation for the advancement of cushion protection technology and the optimization of structure for the safety of military and civilian products.

Materials and methods

In this investigation, the honeycomb paperboard and PE foam are chosen as the base material. The sample manufacturing process entails that the honeycomb paperboard needs to undergo die-cutting, indentation, and folding. Then, white latex is applied to bond the connecting edge (in the same direction as the indentation) of the honeycomb paperboard. Subsequently, the paper honeycomb sandwich tubes with cross-sections of regular quadrangles, pentagons, and hexagons are produced, respectively. Ultimately, the foamed closed-cell polyethylene was made into the blocks following the specified sandwich tube dimensions and subsequently incorporated into the paper honeycomb sandwich tube to obtain the requisite X-direction filled tube (X-DFT) and the Y-direction filled tube (Y-DFT) (as shown in Fig. 1). The units of the honeycomb cells are not filled by the PE form.

To fully inspect the energy absorption properties of the closed-cell PE foam-filled paper honeycomb sandwich tube, in this work, the structures studied are classified into the X-DFT and the Y-DFT. This division is made according to two key parameters: the tubular length direction (X-direction or Y-direction) and the arrangement direction of the regular hexagonal honeycomb cells (Fig. 1a). Due to the different arrangements of honeycomb cells, paper honeycomb sandwich tubes can be classified into X tubes and Y tubes (Fig. 1b, c). Furthermore, regular quadrangles, pentagons, and hexagons are manufactured as tubular cross-section shapes, and classified into X-DFT and Y-DFT, respectively.

Figure 1 presents the structure diagram of a filled tube with a regular hexagonal cross-section. Tubular cross-section edge lengths of 35 mm and 50 mm, and tubular length ratios of 1.4, 2.2, and 3.0 were chosen. The tubular length ratio is the ratio of the tubular length to the edge length of the regular polygonal cross-section[20]. The density of the PE foam was 16.4 kg/m^3, and its thickness was 55 mm. The thickness of the honeycomb paperboard was 10 mm, and its edge length was 5.77 mm. Table 1 provides the basic parameters of the honeycomb paperboard.

As shown in Table 2, three drop heights (30, 50, and 70 cm) and four drop weight masses (7.0, 9.125, 11.275, and 14.550 kg) were designed to create 12 pairs of drop impact conditions[21]. Three drop tests were the experiments repeated for each sample type under similar test conditions. If data was found to be abnormal in the three drop tests, check the sample and redo the three drop tests. The samples are numbered as HT*nd-l*1/*l*2-SF-DH/W, where HT, *n*, *d*, *l*1, *l*2, SF, DH, and W, represent the paper honeycomb tube, the edge number of the polygonal cross-section, the tubular direction, the edge length of the tubular cross-section, the tubular length, single filling, the drop height, and the drop weight mass, respectively. The area of the sample was smaller than the bottom area of the square drop block.

Before the tests, all specimens were preconditioned for 24 h at a relative humidity of 65% and an ambient temperature of 20 °C. The drop impact test method refers to the Chinese national standard GB 8167 "Testing method of dynamic compression for packaging cushioning materials" and the ASTM D 1596 "Standard test method for dynamic shock cushioning characteristics of packaging materials." The DY-3 impact testing machine (made in Xi'an Jiesheng Electronic Technology Co., LTD) was used to exert the drop impact loading on the cross-section of the specimen with a square drop weight, and the impact energy can be adjusted by the drop height and the mass of the drop hammer.

Results

Dynamic compression deformation properties

The axial dynamic compression deformation[22] of the closed-cell PE foam-filled paper honeycomb sandwich tube is shown in Fig. 2. Figure 2a shows a complete collapse deformation, the tubular wall is folded. Figure 2b shows an incomplete collapse deformation, one end of the tubular wall undergoes progressive buckling. Figure 2c compares the compression curves for complete and incomplete deformation. Due to the short drop impact time, the difference in tubular length and impact energy, the filled tubes have the phenomenon of incomplete collapse. At this time, only a part of the filled tube is folded and wrinkled, and the corresponding stress and strain curve is mainly the linear elastic region and plastic platform region, but no densification. Figure 2d–i provides schematic

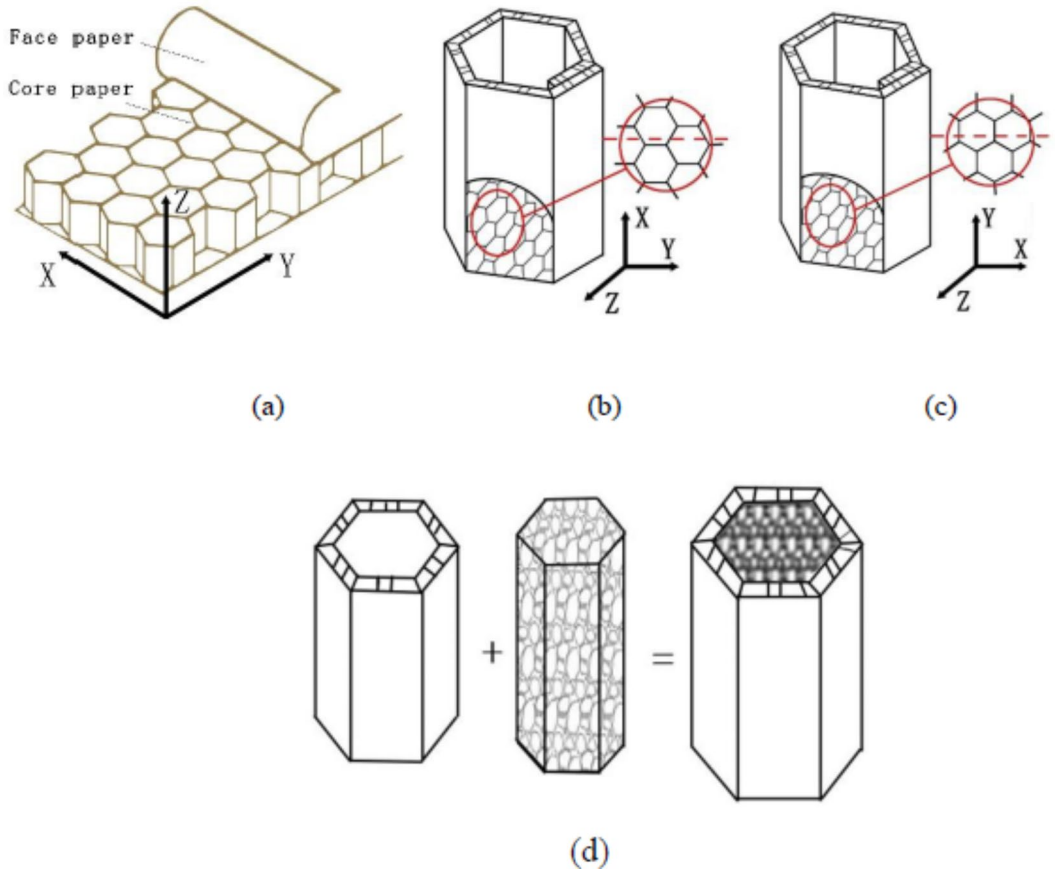

Fig. 1. Geometric description of paper honeycomb sandwich tube filled with PE foam (**a**) honeycomb paperboard, (**b**) X-direction tube, (**c**) Y-direction tube, (**d**) filled tube.

Honeycomb base paper	Grammage (g/m^2)	Thickness (mm)	Tensile strength (N/mm^2)		Ring compression strength (N/m)	
			Transverse	Longitudinal	Transverse	Longitudinal
Face paper	200	0.244	25.33	34.01	1600	1830
Core paper	124	0.218	12.67	27.33	640	819

Table 1. Mechanical properties of honeycomb paperboard.

diagrams of the deformation of the PE foam-filled tubes after drop impact dynamic compression, qualitatively describing the progressive buckling deformation mode of the filled tubes with a tubular cross-section edge length of 50 mm and a tubular length of 110 mm.

We refer to the deformation mode of aluminum foam-filled metal thin-walled round tubes and compare the compression deformation results with those of PE foam-filled regular polygon paper honeycomb sandwich tubes[23–25]. We analyzed the deformation mode of the interaction between the tubular wall and foam for the X-DFT and Y-DFT under axial loading conditions. The main findings obtained from this study are summarized as shown in Fig. 3. For the drop impact dynamic compression conditions, Fig. 3a shows the filled tube was not completely crushed. Due to part of the tube not being crushed, the tube still has a certain cushioning energy absorption effect. Figure 3b shows the deformation mode of the filled tube completely crushed. The tube is completely crushed and unable to perform its cushioning capacity.

The observed deformation modes of the filled tubes present with progressive buckling and folding appearances. As shown in Fig. 4, it can be seen that the axial dynamic compression deformation modes of the X-DFT and Y-DFT exhibit obvious differences.

During dynamic compression, the air within the honeycomb cells will generate a discernible compression force. Upon impact with the drop hammer, the specimen exhibits elastic behavior and rapidly attains the initial peak stress. Subsequently, the specimen begins to yield, displaying gradual buckling and folding. As the tubular wall is subjected to continuous compression, the specimen undergoes a gradual collapse until it reaches a densely compressed state.

Sample type	Drop height (cm)	Drop weight masses (kg)
HT4X	30 (50 and 70)	7.0
		9.125
		11.275
		14.550
HT4Y	30 (50 and 70)	7.0
		9.125
		11.275
		14.550
HT5X	30 (50 and 70)	7.0
		9.125
		11.275
		14.550
HT5Y	30 (50 and 70)	7.0
		9.125
		11.275
		14.550
HT6X	30 (50 and 70)	7.0
		9.125
		11.275
		14.550
HT6Y	30 (50 and 70)	7.0
		9.125
		11.275
		14.550

Table 2. Experimental conditions of axial loading.

Under similar impact conditions, the energy absorbed by the compression of the X-DFT is greater than that of the Y-DFT. Therefore, the cushioning energy absorption effect of the X-DFT is superior to that of the Y-DFT. Honeycomb paperboard exhibits robust resistance to in-plane compression and demonstrates enhanced energy absorption capabilities during dynamic compression deformation. This phenomenon involves the honeycomb cells with progressive buckling and the formation of periodic folds.

The experimental analysis results showed that the drop shock response waveforms of the filled tubes all exhibited half-sine-wave shapes. Compared with the corresponding Y-DFTs, the peak acceleration of the regular quadrangle, pentagon, and hexagon X-DFTs increased by 2.4–18.9%, 5.5–22.2%, and 8.2–21.0%, respectively. The impact duration of the regular quadrangle, pentagon, and hexagon Y-DFTs increased by 1.0–3.6%, 0.7–2.8%, and 0.6–3.5%, respectively, compared to the corresponding X-DFTs.

Energy absorption analysis

Specific energy absorption (SEA) and specific total efficiency (STE) are chosen as key energy-absorbing indicators to analyze the compression load, deformation, and energy-absorbing capacity of filled tubes[26].

SEA is defined as the ratio of total energy absorption (E) to mass (m) before the sample enters densification, which is expressed as follows:

$$\mathrm{SEA} = \frac{E}{m} = \frac{\int_0^{\delta} F ds}{m}, \tag{1}$$

where δ is the compression displacement deformation, and F is the crush load.

STE is defined as the ratio of SEA of unit tubular length (l_2) to initial peak load (F_{max}):

$$\mathrm{STE} = \frac{SEA}{l_2 \cdot F_{max}} = \frac{E}{m} \cdot \frac{1}{l_2} \cdot \frac{1}{F_{max}}. \tag{2}$$

The calculated energy-absorption parameters of the filled tubes are given in Table 3. SEA and STE show a downward trend with the increase of the edge number of tubular cross-sections. The SEA and STE of the X-DFT respectively increase by 25.5–33.1% and 5.7–25.2% compared with the Y-DFT, and the crush force efficiency of the quadrangle X-DFT is closest to the ideal value of one.

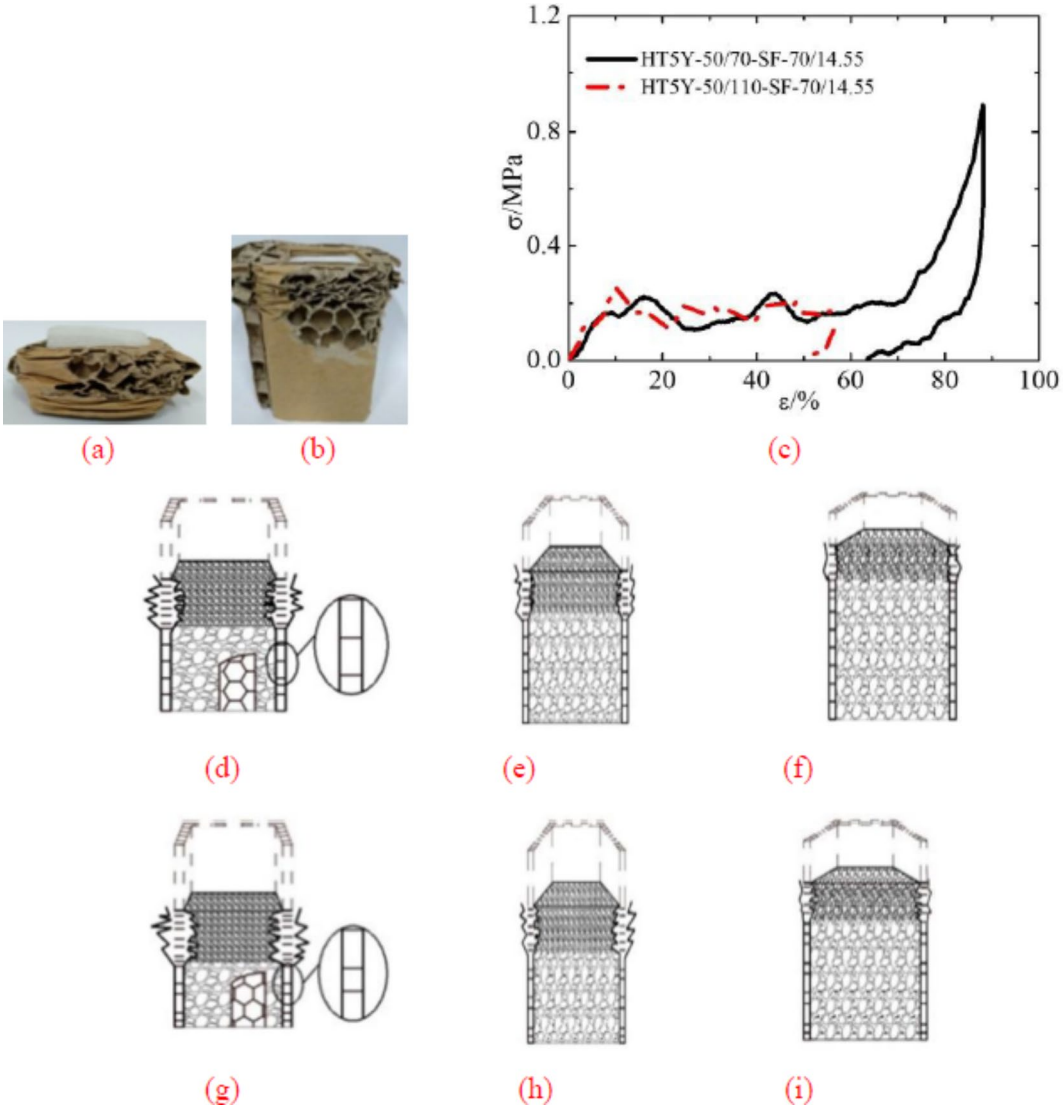

Fig. 2. Dynamic compression deformation diagrams and progressive buckling deformations of the filled tube (**a**) filled tube with complete collapse deformation, where the tubular wall is folded; (**b**) incomplete collapse deformation, where one end of the tubular wall undergoes progressive buckling; (**c**) comparison of compression curves for complete and incomplete deformation; (**d**–**f**) progressive buckling deformations of (**d**) quadrilateral X-DFT, (**e**) pentagonal X-DFT, and (**f**) hexagonal X-DFT; (**g**–**i**) progressive buckling deformations of (**g**) quadrilateral Y-DFT, (**h**) pentagonal Y-DFT, and (**i**) hexagonal Y-DFT.

Influence of tubular direction

Figure 5 presents the calculations of the energy absorption of the filled tube under axial drop impact loading. Compared with the corresponding Y-DFT, the SEAs of the regular quadrangle, pentagon, and hexagon X-DFT increased by 0.6–66.8%, 1.2–73.6%, and 2.7–84.9% (Fig. 5a); and the STEs increased by 2.4–109.2%, 6.3–111.8%, and 10.7–147.5% (Fig. 5b), respectively. The main reason for these differences is that the X-DFT and Y-DFT of paper honeycomb sandwich tubular walls are subject to different force conditions during dynamic compression[27], and they deform under in-plane compression loading along the X-direction and Y-direction of the honeycomb cell, respectively, as shown in Fig. 5c,d.

Influence of tubular cross-section shape

The calculated energy absorption indices of the filled tubes with different tubular cross-section shapes are provided in Table 4. Compared to the regular pentagon and hexagon tubes, the SEA of the regular quadrangle X-DFT increased by 4.4–218.2% and 6.3–299.5%, respectively. Compared to the regular pentagon and hexagon tubes, the SEA of the regular quadrangle X-DFT increased by 4.4–218.2% and 6.9–212.5%, and the STE increased by 6.3–299.5% and 8.1–276.0%, respectively. Compared to the regular pentagon and hexagon tubes, the SEA of the regular quadrangle Y-direction filled tubes increased by 3.1–133.3% and 3.7–220.8%, and the STE increased by 11.5–152.2% and 8.2–232.2%, respectively.

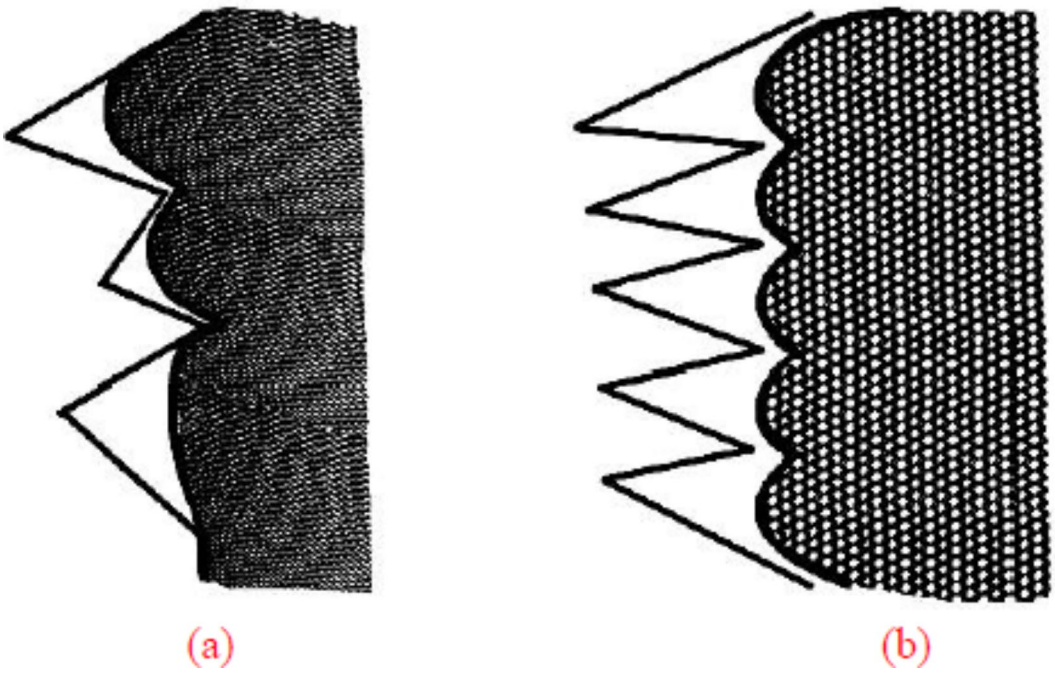

Fig. 3. Mutual deformation modes between tubular wall and foam (**a**) contact and (**b**) not contact.

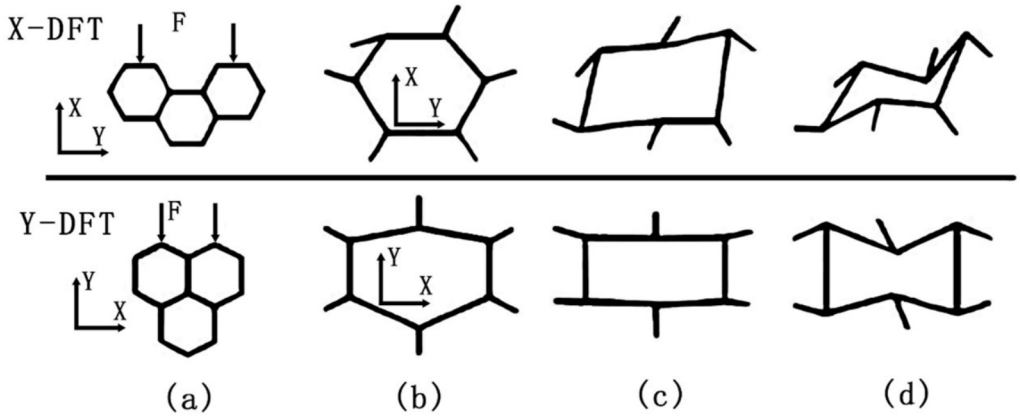

Fig. 4. Deformation modes of X-DFT and Y-DFT (**a**) force direction; (**b**) elastic deformation; (**c**) plastic deformation; (**d**) densification deformation.

Sample type	SEA (J/g)	STE (10^{-2} g^{-1})
HT4X-50/150-SF-12	3.417	1.757
HT4Y-50/150-SF-12	2.661	1.444
HT5X-50/150-SF-12	2.858	1.291
HT5Y-50/150-SF-12	2.147	1.031
HT6X-50/150-SF-12	2.328	0.880
HT6Y-50/150-SF-12	1.855	0.832

Table 3. The parameters of energy absorption.

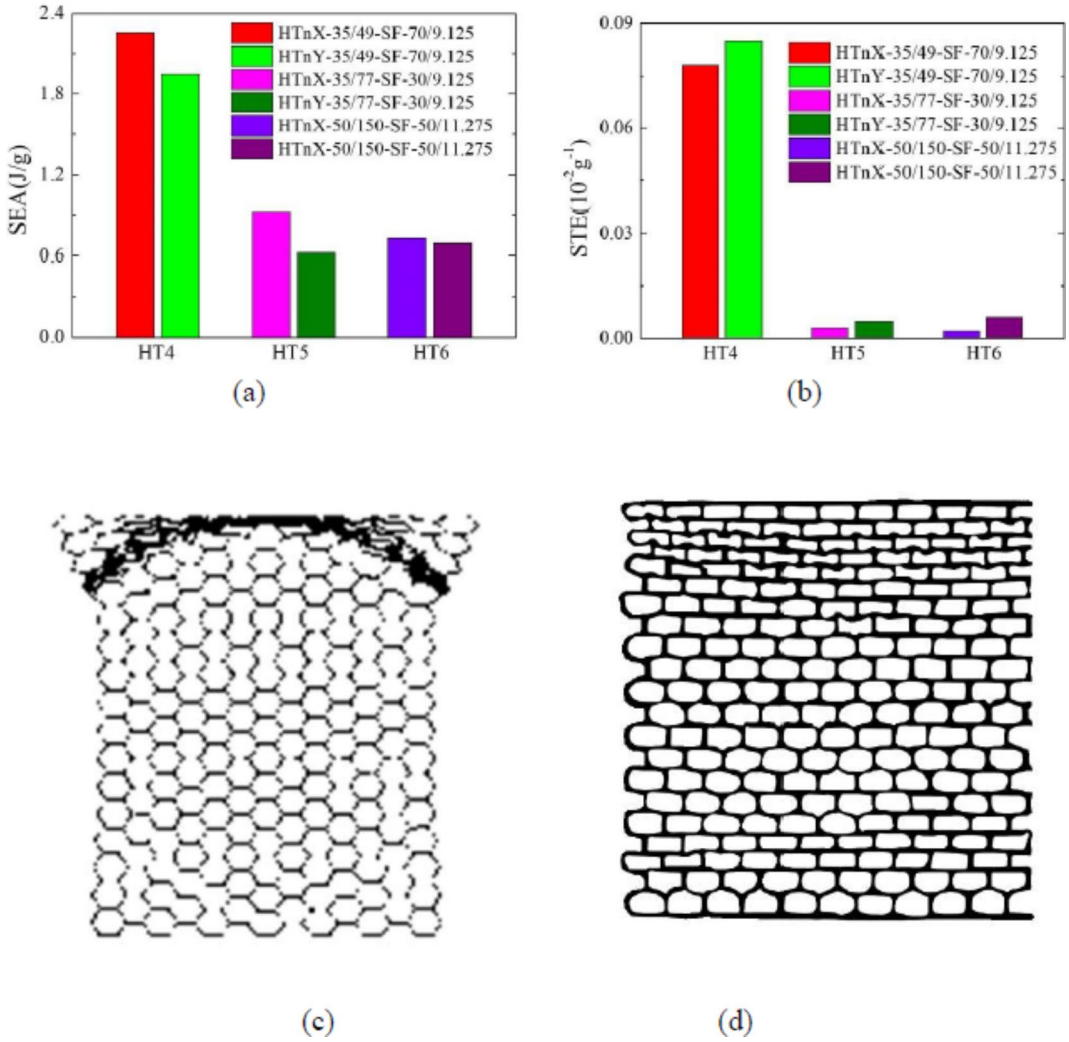

Fig. 5. Comparison of energy absorption and deformations of the tubular wall for different tubular directions (**a**) specific energy absorption, (**b**) specific total efficiency; wall deformations of (**c**) X-DFT and (**d**) Y-DFT.

Sample type	SEA (J/g)	STE (10^{-2} g^{-1})
HT4X-35/105-SF-30/11.275	1.850	0.013
HT5X-35/105-SF-30/11.275	1.326	0.098
HT6X-35/105-SF-30/11.275	0.800	0.007
HT4Y-50/110-SF-70/7	1.667	0.019
HT5Y-50/110-SF-70/7	1.187	0.010
HT6Y-50/110-SF-70/7	1.019	0.008

Table 4. Energy absorbing indices for different tubular cross-section shapes.

Influence of tubular length ratio

The axial dynamic compression curves for the filled tubes with different tubular length ratios are compared in Fig. 6. The initial peak stress of the regular pentagon X-DFT with a tubular length ratio of 1.4 increased by 6.5% and 13.1% compared to those of 2.2 and 3.0, respectively. The initial peak stress of the regular hexagon Y-DFT with the tubular length ratio of 1.4 increased by 16.7% and 23.9% compared to those of 2.2 and 3.0, respectively. The strain of the plastic platform area of the regular hexagon X-DFT with a tubular length ratio of 1.4 increased by 97.2% and 160.5% compared to those of 2.2 and 3.0, respectively. By comparison, the strain of the plastic platform area of the regular hexagon Y-DFT with a tubular length of 1.4 only increased by 67.0% and 97.2% compared to those of 2.2 and 3.0, respectively.

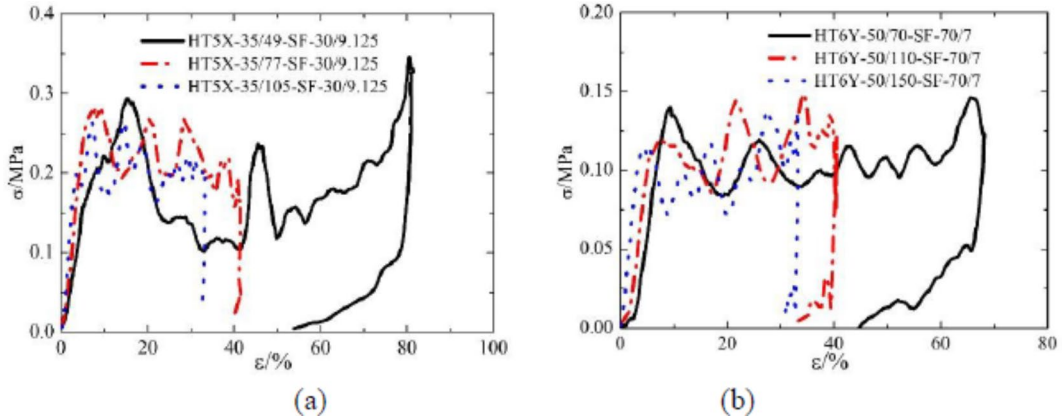

Fig. 6. Comparison of compression curves for different tubular length ratios under drop impact (**a**) X-DFT and (**b**) Y-DFT.

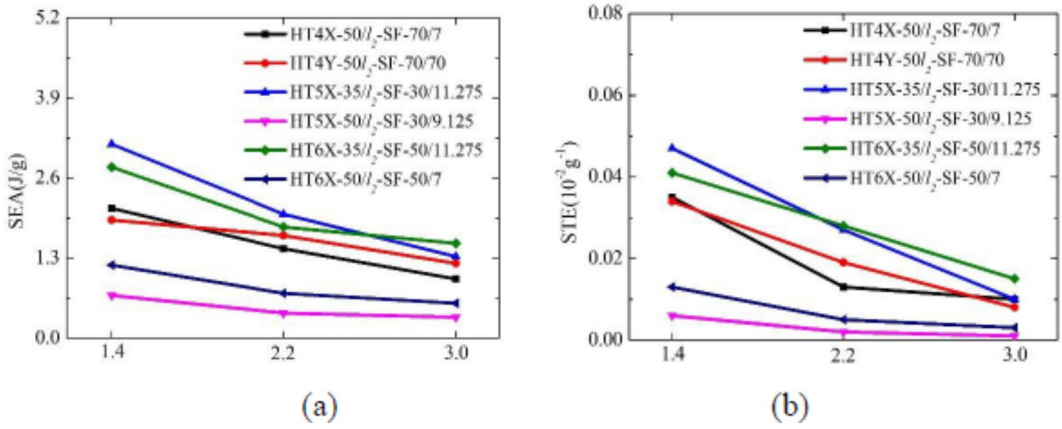

Fig. 7. Comparison of energy absorption for different tubular length ratios (**a**) specific energy absorption and (**b**) specific total efficiency.

Figure 7 compares the dynamic energy absorption of the filled tubes with different tubular length ratios. For the regular quadrangle, pentagon, and hexagon X-DFT and Y-DFT, the tube length ratio of 1.4 showed the highest SEA and STE, followed by 2.2 and then 3.0.

Influence of impact energy

For the axial compression of a tubular structure by drop impact loading, the impact energy is an important external factor that affects not only compression performance but also energy-absorbing capacity. Taking the filled tube with a tubular cross-section edge length of 50 mm and a tubular length ratio of 3.0 as an example, Fig. 8 shows the comparison of the axial drop impact cushioning energy absorption for the filled tube under 12 types of drop impacts.

Compared with an impact energy of 20.6 J (drop height = 70 cm, weight mass = 14.550 kg), the SEAs of the regular quadrangle, pentagon, and hexagon X-DFTs at an impact energy of 99.8 J (drop height = 30 cm, weight mass = 7.0 kg) increased by 547.0%, 339.1%, and 380.3%, whereas those of the corresponding Y-DFTs increased by 259.8%, 766.2%, and 666.6%, respectively. Under the same conditions, the STEs of the X-DFTs increased by 339.7%, 257.5%, and 350.4%, whereas those of the corresponding Y-DFTs increased by 213.7%, 1221.3%, and 464.2%, respectively. These results indicate that the quadrangle tube had the best energy-absorbing capacity.

Discussion

As shown in Fig. 3, the axial dynamic compression deformation mainly includes two cases of complete and incomplete collapse deformation, with progressive buckling and folding characteristics. Figure 3a shows a complete collapse deformation, where the tubular wall exhibits an obvious fold. Figure 3b shows an incomplete collapse deformation, where the upper end of the tubular wall undergoes progressive buckling[23]. For HT5Y-50/70-SF-70/14.55 and HT5Y-50/110-SF-70/14.55 (Fig. 3b), due to the short drop impact time, as well as the difference in tubular length and impact energy, the filled tubes exhibited incomplete collapse, where only a part of the filled tube was folded and wrinkled. The corresponding stress and strain curve was mainly in the linear

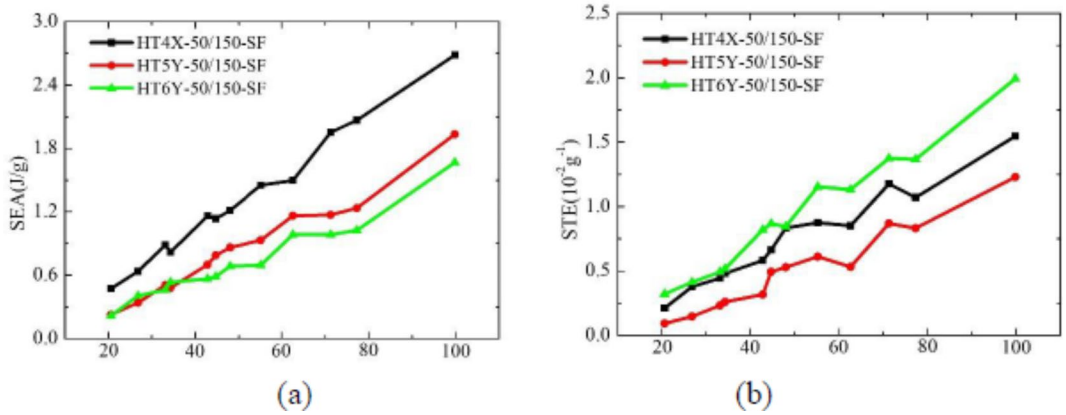

Fig. 8. Comparison of energy absorption for different drop impact energies (**a**) specific energy absorption and (**b**) specific total efficiency.

elastic and plastic regions, with no densification. According to the analysis of the test results, the stress increased rapidly at the end of the compression curve, and the strain value exceeded 83%, indicating complete collapse. There are many factors that could be involved in complete collapse, such as paper honeycomb sandwich tubular cross-section area, tubular length, and impact energy.

Under axial static compression conditions with a constant loading rate, the foam deformed non-uniformly, the tubular wall of the paper honeycomb sandwich tube was compressed to form folds and a portion of the foam was forced into the folds formed by the tubular wall, as shown in Fig. 4a. In this case, the external loading was resisted by the PE foam, the paper honeycomb sandwich tube, and the interaction between the foam and the tubular wall. For the drop impact dynamic compression conditions, if the filled tube was not completely crushed, the foam was also squeezed into the tubular wall folds. For Fig. 4b, after the filled tube was compressed, the foam deformed uniformly. Due to the short compression time, the gas in the paper honeycomb cannot escape quickly and the tubular wall ruptures, causing the PE foam to not contact the paper honeycomb sandwich tubular wall.

The vertical changing regularities of these key energy absorption indexes (SEA and STE of paper honeycomb sandwich tubes filled with PE foam) are consistent with the increase of drop impact mass and impact energy[20,27] (Table 3). The paper honeycomb tubular wall has strong in-plane compression resistance, can absorb more energy, and form wrinkles under drop impact dynamic loading. However, in the same state of drop impact, the energy absorbed by the X-DFT is greater than that of the Y-DFT (Fig. 5). As the edge number of the tubular cross-section increased, SEA and STE decreased significantly (Table 4). As the tubular length ratio increased, the initial peak stress gradually decreased, and as the tubular length ratio increased, the strain in the plastic platform area decreased (Fig. 6). SEA and STE decreased as the tubular length ratio increased. This is because as the tubular length ratio increased, the average crushing load and the initial peak load increased (Fig. 7). As the drop impact energy increased, SEA and STE increased linearly, these results indicate that the quadrangle tube had the best energy-absorbing capacity (Fig. 8).

Structural and material parameters significantly affect the load-bearing and energy-absorbing abilities of foam-filled sandwich tubes[28] (Figs. 5, 6 and 7, and 8). Sandwich tubes exhibit progressive buckling deformation mode in the dynamic compression process of drop impact. The corresponding dynamic compression deformation curves show multiple fluctuation folds, an obvious stress plateau, and a densification trend, and the paper honeycomb shows progressive plastic crushing deformation[29] (Fig. 3c). PE closed-cell foam absorbs energy through compression deformation. Under the dynamic compression of the drop impact, the larger impact energy compresses the air trapped in the compressed paper honeycomb and forms a restoring force on the cell wall.

Conclusions

In this work, a regular polygonal paper honeycomb sandwich tube filled with PE foam was proposed in the design of sandwich tubes to improve energy absorption capacity under axial loading. First, the paper honeycomb sandwich tubes filled with PE foam specimens were manufactured and tested. Then, the crushing strength and yield strength of the X-DFTs and Y-DFTs were compared. Finally, their energy absorption capacity was analyzed in terms of SEA and STE[30].

The results showed that the drop shock response waveforms of the filled tubes were all half-sine wave shapes. Due to the short drop impact time, as well as the difference in tubular length and impact energy, the filled tubes showed incomplete collapse. At that time, only a part of the filled tube was folded and wrinkled, with the corresponding stress and strain curve mainly in the linear elastic region and the plastic platform region, but with no densification. SEA and STE tended to decrease with the increase of the edge number of the tubular cross-section. The crush force efficiency of the quadrangle X-DFT was closest to the ideal value of one. The paper honeycomb tubular wall has strong in-plane compression resistance. Furthermore, the energy absorption capacity of the foam-filled sandwich tube increased and formed wrinkles under drop impact dynamic loading. However, under the drop impact conditions, the X-DFT absorbed more energy than the Y-DFT. Under axial

drop impact loading, the deformation characteristics of the filled honeycomb sandwich tube were mainly crushing deformation mode, and the phenomenon of incomplete crushing also occurred. Although the SEA of the X-DFT was higher than that of the Y-DFT, the STE of the Y-DFT was larger than that of the X-DFT. With the increase of the tubular length ratio or the edge number of the tubular cross-section, SEA and STE both tended to decrease. As the drop impact energy increased, the STE of the filled tubes increased linearly as a whole, and the filled square tubes had the best energy absorption capacity.

Composite tubes have the advantages of large specific strength and stiffness as well as good cushioning and energy-absorbing capacity and are widely used in the field of product packaging protection and safe transportation. In this work, the influence of paper honeycomb sandwich tubes filled with PE foam on the dynamic compression deformation characteristics and energy absorption characteristics of such structures was analyzed, which provides a reference for its application in the field of impact protection and product transportation packaging. This work presents the preliminary work from our research series on the energy absorption capacity of paper honeycomb sandwich tubes filled with PE foam composite tubes. In this study, the energy absorption of the paper honeycomb sandwich tubes filled with PE foam composite tubes is still insufficient, and the combination form of the composite tubes sample and test parameters needs to be optimized, which needs to be further explored in future works.

Data availability

Data is provided within the manuscript .

Received: 16 April 2024; Accepted: 17 September 2024
Published online: 28 September 2024

References

1. Dehghanpour, S. & Nia, A. A. Experimental and numerical study of in-plane loading of thin-walled tubes with different section shapes and wall thickness. *Int. J. Adv. Des. Manuf. Technol.* **15** (3), 89–97 (2022).
2. Taghipoor, H., Ghiaskar, A. & Shavalipour, A. Crashworthiness performance of thin-walled, square tubes with circular hole discontinuities under high-speed impact loading. *Int. J. Crashworthiness*. **27** (6), 1622–1634 (2022).
3. Birman, V. & Kardomateas, G. A. Review of current trends in research and applications of sandwich structures. *Compos. Part. B: Eng.* **142**, 221–240 (2018).
4. Ha, N. S. & Lu, G. A review of recent research on bio-inspired structures and materials for energy absorption applications. *Compos. Part. B: Eng.* **181**, 107496 (2020).
5. Tsushima, N. et al. Geometrically nonlinear static aeroelastic analysis of composite morphing wing with corrugated structures. *Aerosp. Sci. Technol.* **88**, 244–257 (2019).
6. Lin, Y. Y. et al. Thermoplastic laminated composites applied to impact resistant protective gear: structural design and development. *Polymers*. **15** (2023).
7. Azimi, M. B., Asgari, M. & Salaripoor, H. A new homo-polygonal multi-cell structures under axial and oblique impacts; considering the effect of cell growth in crashworthiness. *Int. J. Crashworthiness*. **25** (6), 628–647 (2020).
8. Wu, F. et al. Mechanical properties and energy absorption of composite bio-inspired multi-cell tubes. *Thin-Walled Struct.* **184**, 110451 (2023).
9. Dehghanpour, S. et al. Comparative analysis of energy absorption capacity of single and nested metal matrix composite tubes under quasi-static lateral and axial loading. *J. Solid Mech.* **13** (2), 134–143 (2021).
10. Taghipoor, H. & Eyvazian, A. Quasi-static axial crush response and energy absorption of composite wrapped metallic thin-walled tube. *J. Brazilian Soc. Mech. Sci. Eng.* **44** (4), 158 (2022).
11. Eyvazian, A., Tran, T. N. & Hamouda, A. M. Experimental and theoretical studies on axially crushed corrugated metal tubes. *Int. J. Non-Linear Mech.* **101**, 86–94 (2018).
12. Liu, Z. et al. Axial-impact buckling modes and energy absorption properties of thin-walled corrugated tubes with sinusoidal patterns. *Thin-Walled Struct.* **94**, 410–423 (2015).
13. Yuan, L. et al. Quasi-static impact of origami crash boxes with various profiles. *Thin-Walled Struct.* **141**, 435–446 (2019).
14. Ye, H. et al. Energy absorption behaviors of pre-folded composite tubes with the full-diamond origami patterns. *Compos. Struct.* **221**, 110904 (2019).
15. Taghipoor, H. & Sefidi, M. Energy absorption of foam-filled corrugated core sandwich panels under quasi-static loading. *Proc. Inst. Mech. Eng. Part. L J. Materi. Des. Appl.* **237** (1), 234–246 (2022).
16. Goyal, S. et al. Crashworthiness analysis of foam filled star shape polygon of thin-walled structure. *Thin-Walled Struct.* **144**, 106312 (2019).
17. Kılıçaslan, C. Numerical crushing analysis of aluminum foam-filled corrugated single- and double-circular tubes subjected to axial impact loading. *Thin-Walled Struct.* **96**, 82–94 (2015).
18. Huang, K. et al. Energy absorption properties of composite sandwich tubes with pre-folded cores. *Compos. Struct.* **294**, 115737 (2022).
19. Zhang, Y. et al. Dynamic impact response of aluminum honeycombs filled with expanded polypropylene foam. *Compos. Part. B: Eng.* **156**, 17–27 (2019).
20. Guo, Y. et al. Effect of polyethylene foam on dynamic cushioning energy absorption of paper corrugation tubes. *J. Mech. Sci. Technol.* **36** (4), 1857–1865 (2022).
21. Guo, Y. et al. Cushioning energy absorption of regular polygonal paper corrugation tubes under axial drop impact. *Sci. Eng. Compos. Mater.* **27** (1), 469–483 (2020).
22. Cheng, F. et al. Dynamic compression deformation behavior of laser directed energy deposited $\alpha+\beta$ duplex titanium alloy with basket-weave morphology. *Addit. Manuf.* **61**, 103336 (2023).
23. Yan, K. et al. Crushing characteristics on square tubes under progressive buckling. *Int. J. Steel Struct.* **23** (1), 139–153 (2023).
24. Teng, L., Qingtian, D. & Xinbo, L. Energy absorption and deformation modes of several thin-walled tubes under dynamic compression. *Structures*. **54**, 890–897 (2023).
25. Ji, M. et al. Dynamic cushioning energy absorption of paper composite sandwich structures with corrugation and honeycomb cores under drop impact. *J. Sandw. Struct. Mater.* **24** (2), 1270–1286 (2021).
26. Baroutaji, A., Sajjia, M. & Olabi, A. On the crashworthiness performance of thin-walled energy absorbers: recent advances and future developments. *Thin-Walled Struct.* **118**, 137–163 (2017).
27. Xiang, Y., Yu, T. & Yang, L. Comparative analysis of energy absorption capacity of polygonal tubes, multi-cell tubes and honeycombs by utilizing key performance indicators. *Mater. Design*. **89**, 689–696 (2016).

28. He, Y. et al. Design and mechanical properties analysis of hexagonal perforated honeycomb metamaterial. *Int. J. Mech. Sci.* **270**, 109091 (2024).
29. Zhao, M. et al. Plastic behavior of the foam-filled sandwich beam with circular tube core under transverse loading. *Eng. Struct.* **268**, 114801 (2022).
30. Lu, F. D. et al. A phenomenological constitutive modelling of polyethylene foam under multiple impact conditions. *Packag. Technol. Sci.* **32** (2019).

Acknowledgements
We are grateful to the "Intelligent Transportation Packaging and Logistics Protection Technology" team led by Professor Yanfeng Guo who offered help during the experiment, and Xiaorong Zhang who offered review and editing.

Author contributions
XD (First Author): Conceptualization, funding acquisition, formal analysis, manuscript composition. YG (Corresponding Author): Methodology, resources, funding acquisition, writing—review and editing. YF: Experimental design, resources, supervision, project administration. XH: Carrying out measurements, visualization, data curation, original draft. QW: Investigation, software, validation, data curation. All authors reviewed the manuscript.

Declarations

Competing interests
The authors declare no competing interests.

Additional information
Correspondence and requests for materials should be addressed to X.D. or Y.G.

Reprints and permissions information is available at www.nature.com/reprints.

Publisher's note Springer Nature remains neutral with regard to jurisdictional claims in published maps and institutional affiliations.